



The role of lesion hypointensity on gadobenate dimeglumine–enhanced hepatobiliary phase MRI as an additional major imaging feature for HCC classification using LI-RADS v2018 criteria

Yao Zhang¹ · Wenjie Tang¹ · Sidong Xie¹ · Jingbiao Chen¹ · Linqi Zhang¹ · Dailin Rong¹ · Sichi Kuang¹ · Bingjun He¹ · Jin Wang¹

Received: 18 October 2020 / Revised: 14 January 2021 / Accepted: 17 February 2021 / Published online: 29 March 2021
© European Society of Radiology 2021

Abstract

Objectives To determine the value of lesion hypointensity in the hepatobiliary phase (HBP) on gadobenate dimeglumine–enhanced MRI as an additional major imaging feature for diagnosis of hepatocellular carcinoma (HCC) using LI-RADS v2018 criteria.

Methods Between March 2016 and August 2018, 235 patients with 250 hepatic nodules at high risk of HCC underwent gadobenate dimeglumine–enhanced MRI. Two radiologists independently evaluated the imaging features and classified the nodules based on LI-RADS v2018 criteria, and their consensus data were used to calculate the diagnostic performance of LI-RADS categories. Two modified LI-RADS definitions were as follows: (1) LI-RADS-m1: HBP hypointensity as an additional major feature; (2) LI-RADS-m2: HBP hypointensity as an alternative to “enhancing capsule” as an additional major feature. The diagnostic performance of LR-5 categories was compared using McNemar’s test.

Results The sensitivity and specificity for LR-5 classification using original LI-RADS v2018 criteria were 78.1% and 96.3%, respectively. Significantly improved sensitivity (82.7%; $p = 0.004$) with unchanged specificity (96.3%; $p = 1.00$) was seen for LR-5 classification using LI-RADS-m1. Similar sensitivity and specificity (82.7% and 96.3%, respectively) were also seen using LI-RADS-m2. Significantly improved sensitivity (79.5% vs. 64.0%; $p = 0.031$) with unchanged specificity (96.2% vs. 96.2%, $p = 1.00$) was seen using both LI-RADS-m1 and LI-RADS-m2 compared to the original LI-RADS v2018 for 39 HCC nodules measuring 10–19 mm.

Conclusions Lesion hypointensity on gadobenate dimeglumine–enhanced HBP MRI may improve sensitivity for LR-5 classification beyond that achievable using conventional LI-RADS v2018 criteria. Lesion hypointensity may prove a suitable alternative imaging feature to enhancing capsule for accurate LR-5 classification.

Key Points

- Including lesion hypointensity in the HBP as an additional major feature improved sensitivity for LR-5 classification on gadobenate dimeglumine–enhanced MRI.
- Lesion hypointensity in the HBP can replace “enhancing capsule” as an additional major feature for LR-5 classification without impairing specificity.

Keywords Liver neoplasms · Carcinoma, hepatocellular (HCC) · Magnetic resonance imaging (MRI) · Gadobenic acid

Yao Zhang and Wenjie Tang contributed equally to this work.

✉ Jin Wang
wangjin3@mail.sysu.edu.cn

¹ Department of Radiology, the Third Affiliated Hospital, Sun Yat-sen University (SYSU), No 600, Tianhe Road, Guangzhou, Guangdong 510630, People’s Republic of China

Abbreviations

AASLD	American Association for the Study of Liver Diseases
APHE	Arterial hyperenhancement
cHCC-CCA	Combined hepatocellular-cholangiocarcinoma
ECA	Extracellular agent
FNR	False-negative rate

FPR	False-positive rate
GBCA	Gadolinium-based contrast agent
Gd-EOB-MRI	Gadoxetic acid-enhanced MRI
HBP	Hepatobiliary phase
HBV	Hepatitis B virus
HCC	Hepatocellular carcinoma
HGDNs	High-grade dysplastic nodules
iCCA	Intrahepatic cholangiocarcinoma
LI-RADS	Liver Imaging Reporting and Data System
NPV	Negative predictive value
OATP	Organic anion-transporting polypeptide
PPV	Positive predictive value

Introduction

Hepatocellular carcinoma (HCC) is the fifth most common tumor worldwide and the second most common cause of cancer-related death [1–3]. Unfortunately, the prognosis for patients with advanced HCC remains poor [4]. Consequently, the accurate early detection, diagnosis, and staging of patients at increased risk for HCC are vital. The Liver Imaging Reporting and Data System v2018 (LI-RADS v2018 [5]) is the guideline most frequently followed by practitioners [6]. The guideline categorizes detected lesions as LR-1 or LR-2 (definitely or probably benign), through LR-3 (intermediate) to LR-4 or LR-5 (probably or definitely HCC), reserving LR-M for malignant lesions that are not definitely HCC. Only lesions classified as LR-5 are considered definitely HCC for which no further confirmation is needed [1, 7]. Hence, patients with lesions classified as LR-5 at initial characterization can potentially undergo appropriate treatment sooner. Upon its development, LI-RADS version 2018 was adopted by the American Association for the Study of Liver Diseases (AASLD) for 2018 HCC clinical practice guidance [1, 7]. Meanwhile, liver-specific hepatobiliary contrast agents were incorporated to evaluate ancillary features [7, 8]. Unfortunately, despite accumulated experience and considerable improvements in the imaging technology, the diagnostic sensitivity for HCC, especially for small HCC, is still comparatively low (approximately 71%) due to frequent atypical vascular profiles [9, 10].

Hepatobiliary phase (HBP) imaging on hepatobiliary contrast agent-enhanced MRI is considered helpful for detecting early HCC and discriminating HCC from high-grade dysplastic nodules (HGDNs) [11–13]. Moreover, HBP hypointensity on hepatobiliary contrast agent-enhanced MRI demonstrates greater diagnostic sensitivity for HCC compared with that achieved with extracellular agent (ECA)-enhanced MRI [14–16]. Several studies have revealed that HBP hypointensity on gadoxetic acid-enhanced MRI (Gd-EOB-MRI) as an alternative to the washout or as an extension of washout into the HBP

allows improved sensitivity for the diagnosis of HCC [14, 17–19]. However, hypointensity in the HBP is also seen in certain benign observations (e.g., hemangioma) and non-HCC malignancies (e.g., intrahepatic cholangiocarcinoma [iCCA]) that have reduced or absent expression of the organic anion-transporting polypeptide (OATP) [8, 20]. Therefore, controversy surrounds the notion that the HBP as an alternative to the washout or extension of washout to the HBP can reduce the diagnostic specificity of HCC [20]. Enhancing capsule is considered a highly specific imaging feature for the diagnosis of HCC [21]. However, it frequently overlaps with other typical dynamic radiological hallmarks, which may limit its contribution to improving diagnostic sensitivity [21, 22]. Moreover, several studies have reported low interobserver agreement for the recognition of enhancing capsule, which could be a more important problem [7, 23, 24]. Therefore, the incremental benefit of the enhancing capsule for LI-RADS categorization has been questioned.

Gadobenate dimeglumine is a gadolinium-based contrast agent (GBCA) that combines the properties of a conventional extracellular agent with those of a GBCA targeted specifically to the liver [25]. Numerous studies have confirmed the performance of both dynamic and HBP imaging with gadobenate dimeglumine for the detection and characterization of focal liver lesions [26–28]. However, whereas many studies have investigated LI-RADS using ECA- or gadoxetic acid-enhanced MRI, relatively few studies have explored LI-RADS with gadobenate dimeglumine-enhanced MRI. We hypothesized that HBP hypointensity on gadobenate dimeglumine-enhanced MRI could be considered an additional major feature for the diagnosis of HCC and could even replace the enhancing capsule as a major feature. Therefore, the aim of our study was to determine whether lesion hypointensity on HBP imaging with gadobenate dimeglumine could be considered an alternative to the enhancing capsule as a major feature for the diagnosis of HCC using LI-RADS v2018 criteria in patients suspected of harboring HCC.

Materials and methods

Patients

This retrospective study received Institutional Review Board approval and the requirement for patient informed consent was waived. Between March 2016 and August 2018, 943 patients aged ≥ 18 years at high risk of HCC underwent gadobenate dimeglumine-enhanced MRI (Fig. 1). Among these 943 patients, 317 had chronic hepatitis B virus (HBV) infection or liver cirrhosis. These patients were considered eligible for inclusion in the study. Subsequently, 82 patients were excluded from the analysis. Patients were excluded if the

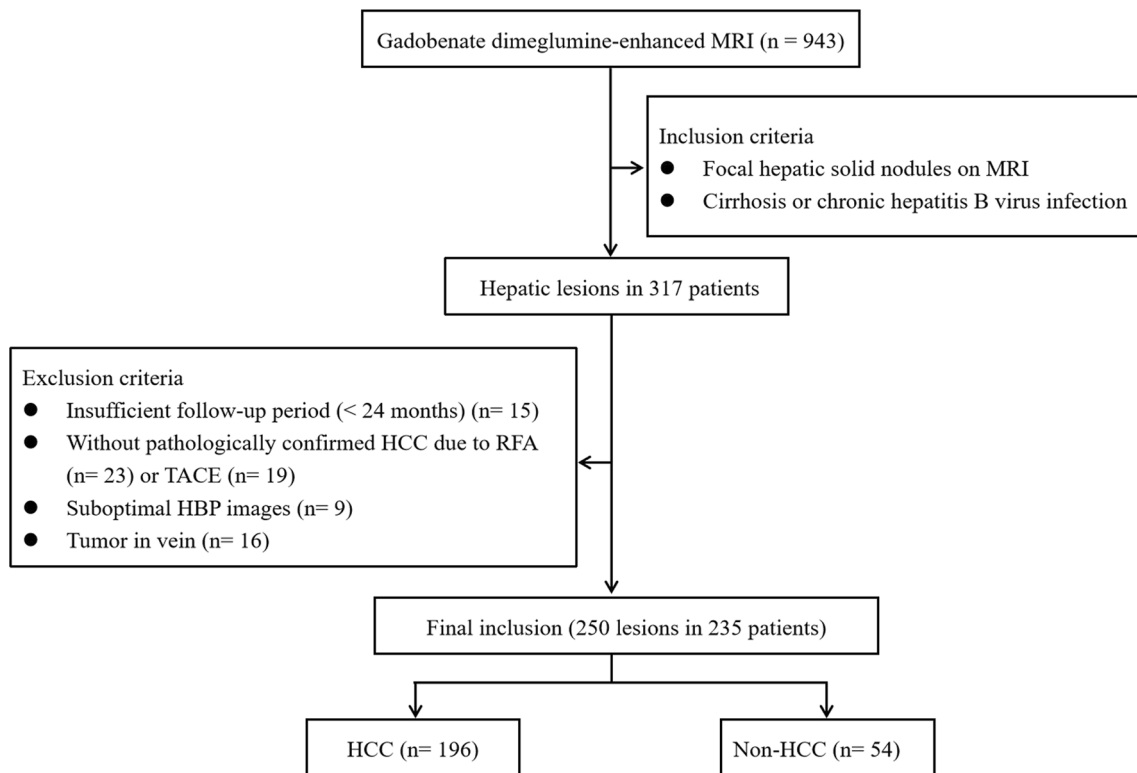


Fig. 1 Flowchart of inclusion and exclusion criteria. MRI, magnetic resonance imaging; HCC, hepatocellular carcinoma; RFA, radio-frequency ablation; TACE, transcatheter arterial chemoembolization; HBP, hepatobiliary phase

follow-up period was < 24 months ($n = 15$), if the final diagnosis was based solely on transcatheter arterial chemoembolization ($n = 19$), or radio-frequency ablation without biopsy ($n = 23$), if the patients had tumor in vein ($n = 16$), or if HBP images were suboptimal ($n = 9$). If multiple hepatic nodules were found, the study coordinator (J.W., with more than 20 years of experience in abdominal MRI) annotated the segmental location of the lesions for analysis (up to three for each patient). A total of 250 nodules in 235 patients were evaluated.

MRI examination

Liver MRI was performed at 3.0 T (Discovery MR750, GE Healthcare; $n = 136$) or 1.5 T (Optima MR360, GE Healthcare; $n = 99$). Both scanners were equipped with an eight-channel phased-array body coil. The routine liver MRI protocol used for all patients included an axial respiratory-triggered fat-saturated T2-weighted fast spin-echo sequence, respiratory-triggered diffusion-weighted imaging with a single-shot echo-planar sequence with b values of 0 and 800 mm^2/s , a breath-hold axial in-phase and out-of-phase T1-weighted LAVA-Flex sequence, and a fat-saturated T1-weighted LAVA-Flex sequence acquired during a single breath-hold before contrast administration (unenhanced) and following contrast administration during the post-contrast dynamic (arterial phase, portal-venous phase, and delayed

phase) and hepatobiliary phases. Contrast-enhanced images were acquired after administration of the gadobenate dimeglumine (MultiHance; Bracco) at a dose of 0.1 mmol/kg body weight. Contrast injection was performed using a dual-head bolus power-injector (Spectris Solaris EP; Medrad) at a rate of 2.0 mL/s , followed by a 20-mL saline injection at the same rate. Arterial phase images were obtained 7–8 s after the detection of contrast arrival in the distal thoracic aorta by means of an MR monitoring system. PVP, DP, and HBP images were then acquired at 60 s, 3 min, and 2–3 h, respectively, after contrast injection. Detailed MRI parameters are described in Supplementary Table 1.

Image analysis

Two radiologists (W.T. and Y.Z., with 15 and 4 years of experience in abdominal MRI, respectively) evaluated all MR images from the 235 included patients. The two readers were informed that all patients were at high risk for HCC and were aware of the location of the target lesion. However, both were fully blinded to the pathology results and to the clinical presentation of the patients. Image assessment utilized the LI-RADS v2018 lexicon (7, 8). Tumor size was measured on axial images in the imaging phase in which the margin was most clearly visible. However, arterial phase images were avoided wherever possible to prevent the inclusion of possible perilesional enhancement in the assessment. Major features of

HCC (i.e., non-rim arterial hyperenhancement [APHE], non-peripheral washout, and enhancing capsule) were independently assessed by the reviewers based on definitions presented in the LI-RADS v2018 lexicon (5, 8). Threshold growth was not analyzed in this study since prior examinations were not available for comparison. Then, lesion hypointensity in the HBP was evaluated. This was defined as lesion intensity that was less than that of the surrounding hepatic parenchyma in whole or in part in the HBP (5, 8). After image evaluation was performed, a specific LI-RADS category was assigned, using only the major imaging features of HCC. Patients were evaluated and LI-RADS categories were assigned by the two radiologists independently. Thereafter, inter-reader agreement was determined regarding the imaging features and LI-RADS categories. Any discrepancies between the two readers to determine imaging features and assign a specific LI-RADS category were subsequently resolved by reevaluation of the images in consensus.

Diagnostic performance

The diagnostic performance of gadobenate dimeglumine-enhanced MRI for the correct classification of lesions as LR-5 based on LI-RADS v2018 major features was determined in terms of sensitivity, specificity, accuracy, false-negative rate (FNR), false-positive rate (FPR), positive predictive value (PPV), and negative predictive value (NPV). After excluding other categories (LR-1, LR-2, and LR-M), observations were recategorized according to the following modified LI-RADS versions and the diagnostic performance of gadobenate dimeglumine-enhanced MRI was reevaluated. The first modification (LI-RADS-m1) considered lesion hypointensity in the HBP as an additional major feature. The second modification (LI-RADS-m2) considered lesion hypointensity in the HBP as an alternative major feature to “enhancing capsule.”

Histopathologic diagnosis

Histopathologic diagnosis of lesions after surgical resection or biopsy was used as the standard of reference. Histopathologic analysis was performed by a single pathologist (Y.L.) with more than 5 years of experience in liver pathology.

Statistical analysis

McNemar’s test was used to compare the sensitivity and specificity of gadobenate dimeglumine-enhanced MRI for the correct classification of LR-5 lesions based on LI-RADS-m1 and LI-RADS-m2 criteria with values obtained using the original LI-RADS v2018 criteria. Subgroup analyses were performed for lesions 10–19

mm in size and for lesions ≥ 20 mm in size. Kappa (κ) statistics were used to determine inter-reader agreement for major features and LI-RADS categorization. The findings were interpreted as slight agreement for κ values of 0.01–0.20, fair agreement for 0.21–0.40, moderate agreement for 0.41–0.60, substantial agreement for 0.61–0.80, and excellent agreement for 0.81–0.99. Statistical analyses were performed using SPSS, version 20 (IBM). A p value < 0.05 was considered statistically significant.

Results

Patient characteristics and pathologic findings

The 235 patients evaluated included 201 men (86%) and 34 women (14%) with a mean (\pm standard deviation) age of 51.4 \pm 11.3 years (Table 1). For most patients (223 [94.9%]), hepatitis B was the principal cause of chronic liver disease. A total of 157/235 (66.8%) patients had liver cirrhosis: 131 according to histopathology and 26 according to the radiologists’ interpretation in consensus.

A total of 250 nodules with a mean size of 32 mm (range, 4–176 mm) were evaluated. Subsequent evaluation confirmed 196 HCC lesions and 54 non-HCC lesions. Among the 54 non-HCC lesions, 15 malignant lesions were confirmed by histopathology as combined hepatocellular-

Table 1 Clinical characteristics of the 235 study subjects

Characteristics	Value
Age* (years)	51.4 (\pm 11.3)
Sex	
Male	201 (85.5%)
Female	34 (14.5%)
Etiology of liver disease	
Hepatitis B	223 (95%)
Hepatitis C	6 (2.6%)
Alcohol	4 (1.7%)
Non-alcoholic fatty liver disease	2 (0.9%)
Cirrhosis	
Presence	157 (66.8%)
Absence	78 (33.2%)
Tumor size, mm	32 (4–176)
AFP level, ng/mL	36.7 (0–121000)
Child-Pugh	
A	226 (96%)
B	9 (4%)

Note: Unless otherwise indicated, data are shown as the median and range or numbers with percentages in parentheses

AFP, α -fetoprotein

*Presented as the mean and standard deviation (SD)

cholangiocarcinoma (cHCC-CCA; $n = 5$), iCCA ($n = 6$), and metastases ($n = 4$). The other 39/54 lesions were benign. These were confirmed either by histopathology ($n = 3$) or by characteristic imaging features and stability or disappearance at 24-month follow-up imaging ($n = 36$) as hemangioma ($n = 15$), arteriportal shunt ($n = 6$), dysplastic nodule (DN) or regenerative nodule (RN) ($n = 14$), focal nodular hyperplasia (FNH) ($n = 2$), cyst ($n = 1$), and abscess ($n = 1$). The 15 hemangiomas and 2 FNHs were diagnosed by means of characteristic enhancement patterns in the dynamic phase after gadobenate dimeglumine administration. Overall, 65 nodules (including 39 HCCs) measured 10–19 mm, and 185 nodules (including 157 HCCs) measured ≥ 20 mm.

LI-RADS categories

The LI-RADS categories assigned to lesions based on gadobenate dimeglumine-enhanced MRI are shown in Table 2. Of the 196 HCC lesions in the lesion population, 153 (78.1%) were categorized as LR-5, 11 (5.6%) as LR-4, 8 (4.1%) as LR-3, and 24 (12.2%) as LR-M. No HCC lesions were classified as LR-1 (false negative) or LR-2. Conversely, of the 54 non-HCC lesions, 15 (27.8%) were classified as LR-M, 13 (24.1%) as LR-1, 11 (20.4%) as LR-2, and 9 (16.7%) as LR-3. Four non-HCC lesions were classified as LR-4, and only 2 (1 dysplastic nodule and 1 cHCC-CCA) were classified as LR-5 (false positive).

Thirteen of 250 (5.2%) lesions were assigned a different category based on the original LI-RADS v2018 criteria compared with the modified LI-RADS (LI-RADS-m1 and LI-RADS-m2) criteria. Six of 17 (35.3%) LR-3 lesions and three of 15 (20%) LR-4 lesions based on LI-RADS v2018 were reclassified as LR-5 using the modified LI-RADS (both LI-RADS-m1 and LI-RADS-m2), and all nine lesions were confirmed to be HCC. Four of 17 (23.5%) LR-3 lesions according to LI-RADS v2018 were reclassified as LR-4 using the modified LI-RADS (both LI-RADS-m1 and LI-RADS-m2), and all four were DNs or RNs.

Diagnostic performance

The diagnostic performance of gadobenate dimeglumine-enhanced MRI for the correct classification of LR-5 lesions based on the original LI-RADS v2018 criteria and the modified LI-RADS (LI-RADS-m1 and LI-RADS-m2) criteria is shown in Table 3. Nine additional HCC lesions (9/196 [4.6%]) were classified as LR-5 with the addition of lesion hypointensity in the HBP as an additional major feature (LI-RADS-m1), increasing the sensitivity for a correct LR-5 classification from 78.06 to 82.65% ([153/196 to 162/196 lesions]; $p = 0.004$). A similar increase in sensitivity for a correct LR-5 classification (78.06 to 82.65%; $p = 0.004$) was obtained when replacing “enhancing capsule” with lesion hypointensity in the HBP as a major feature (Figs. 2 and 3). In neither case was specificity impaired (52/54 lesions; 96.3%; all evaluations; $p = 1.0$). Subgroup analysis showed that the principal benefit was for lesions 10–19 mm in size (Table 4). Six additional small lesions were classified as LR-5, increasing the sensitivity from 64.1 to 79.49% ([25/39 to 31/39 lesions]; $p = 0.031$) compared with only 3 additional lesions of ≥ 20 mm (increase in sensitivity from 81.53% [128/157 lesions] to 83.44% [131/157 lesions]; $p = 0.25$). Again, no differences in specificity were noted (25/26 small lesions; 96.15%; $p = 0.1$, all evaluations; 27/28 large lesions; 96.43%; $p = 0.1$, all evaluations).

LI-RADS imaging features and LR-5 categorization: inter-reader agreement

Inter-reader agreement was substantial to excellent, with κ values ranging from $\kappa = 0.621$ to $\kappa = 0.890$ for all assessed features (Supplementary Table 2). Inter-reader agreement for the diagnostic performances for the LR-5 categorization across the different LI-RADS versions was almost perfect, with all κ values greater than 0.80 (Supplementary Table 2).

Table 2 LI-RADS categories of hepatic lesions on gadobenate dimeglumine-enhanced MRI

	HCC ($n = 196$)	Non-HCC ($n = 54$)	Non-HCC for each LI-RADS category
LI-RADS v 2018			
LR-5	153	2	DN ($n = 1$), cHCC-CCA ($n = 1$)
LR-4	11	4	FNH ($n = 2$), DN or RN ($n = 2$)
LR-3	8	9	DN or RN ($n = 9$)
LR-2	0	11	DN or RN ($n = 2$), APS ($n = 2$), hemangioma ($n = 7$)
LR-1	0	13	APS ($n = 4$), hemangioma ($n = 8$), cyst ($n = 1$)
LR-M	24	15	iCCA ($n = 6$), cHCC-CCA ($n = 4$), metastasis ($n = 4$), abscess ($n = 1$)

DN, dysplastic nodule; cHCC-CCA, combined hepatocellular-cholangiocarcinoma; FNH, focal nodular hyperplasia; RN, regenerative nodule; APS, arteriportal shunt; iCCA, intrahepatic cholangiocarcinoma

Table 3 The diagnostic performance of gadobenate dimeglumine–enhanced MRI for the correct classification of LR-5 lesions based on the original LI-RADS v2018 and modified LI-RADS ($n = 250$)

	Sensitivity (%)	Specificity (%)	Accuracy (%)	FNR (%)	FPR (%)	PPV (%)	NPV (%)
LI-RADS v2018	78.06 (153/196)	96.30 (52/54)	82 (205/250)	21.94 (43/196)	3.7 (2/54)	98.71 (153/155)	54.74 (52/95)
LI-RADS-m1	82.65 (162/196)	96.30 (52/54)	85.6 (214/250)	17.35 (34/196)	3.7 (2/54)	98.78 (162/164)	60.47 (52/86)
LI-RADS-m2	82.65 (162/196)	96.30 (52/54)	85.6 (214/250)	17.35 (34/196)	3.7 (2/54)	98.78 (162/164)	60.47 (52/86)
p^*	0.004	1.0					

* p values, LI-RADS-m1 and LI-RADS-m2 compared with LI-RADS v2018 using McNemar's test

Numbers in parentheses were used to calculate percentages

HCC, hepatocellular carcinoma; LI-RADS, Liver Imaging Reporting and Data System; LI-RADS-m1, modified LI-RADS by the addition of HBP hypointensity as a major feature; LI-RADS-m2, modified LI-RADS by replacing enhancing capsule with HBP hypointensity as the major feature; FNR, false-negative rate; FPR, false-positive rate; PPV, positive predictive value; NPV, negative predictive value

Discussion

Our study aimed to determine whether lesion hypointensity on HBP imaging with gadobenate dimeglumine can be considered an alternative to the enhancing capsule as a major feature for the diagnosis of HCC using LI-RADS v2018 criteria in patients suspected of having HCC. Our results show that the sensitivity for classifying HCC as LR-5 increases significantly from 78.06% based on original LI-RADS v2018 criteria to 82.65% ($p = 0.004$) when hypointensity in the HBP is included as an additional major imaging feature on gadobenate dimeglumine–enhanced MRI. Moreover, the increase in sensitivity is achieved without impacting specificity (96.3% vs. 96.3%). Furthermore, we have showed that the same high sensitivity and specificity (82.65% and 96.3%, respectively) is obtained when lesion hypointensity in the HBP is substituted for enhancing capsule as an additional major imaging feature. The improvement in sensitivity was more evident for lesions 10–19 mm in size (increase in sensitivity from 64.1% to 79.49%) than for lesions of ≥ 20 mm (increase in sensitivity from 81.53% to 83.44%). Previously, Cortis et al [16] similarly demonstrated increases in sensitivity from 53.2% to 75.8% for lesions of ≥ 20 mm and from 53.5% to 62.1% for lesions of 10–19 mm when lesion hypointensity in the HBP was included as an additional major feature to washout in the PVP/DP in cirrhotic patients with hypervascular HCC. Our findings in patients primarily with chronic hepatitis B support those of Cortis et al [16], whose population comprised patients with liver cirrhosis.

Many studies have shown that HBP hypointensity on liver-specific contrast agent–enhanced MRI significantly increases the diagnostic sensitivity for the diagnosis of HCCs [14–16, 29]. Furthermore, a few studies have

recently reported that hypointensity in the HBP is an alternative to the washout or extension of washout to the HBP for diagnosing HCC on Gd-EOB-MRI, with increased sensitivities ranging from 75.3% to 96% [14, 17–19]. These findings are consistent with our results, with the highest sensitivity of 82.65% achieved when adding hypointensity in the HBP to the major features of LI-RADS on gadobenate dimeglumine–enhanced MRI. However, when washout was extended to the HBP on Gd-EOB-DTPA-enhanced MRI, the specificity was reduced [17]. The specificity found in our study was not significantly affected. This is likely because the dynamic phases of gadobenate dimeglumine–enhanced MRI are different from those of gadoxetic acid as a result of the different pharmacokinetics [28, 30, 31]. Given the better visualization of major features during the dynamic phase on gadobenate dimeglumine–enhanced MRI compared to gadoxetate-enhanced MRI [30, 32], our results suggest that gadobenate dimeglumine may be the GBCA of choice for the elaboration of nodules in patients at increased risk for HCC.

Of notable interest is that the same high sensitivity and specificity were achieved when lesion hypointensity in the HBP was included as an additional major feature in place of “enhancing capsule.” In support of our findings, Ehman et al [23] reported that the presence of the enhancing capsule was not helpful for upgrading the LI-RADS classification of all larger LR-4 lesions. HCC capsules comprise two layers: the inner layer, which includes the fibrous component, and the outer layer, which is composed of newly formed bile ducts and small vessels [33, 34]. The enhancing capsule is defined as having a smooth and uniform margin around the lesion, which usually presents as an enhancing rim on the PVP or DP image [7]. In HCCs without a capsule, the enhancing rim on dynamic enhanced MR images may reflect the

Table 4 Subgroup analysis of the diagnostic performance of gadobenate dimeglumine-enhanced MRI for correct classification of LR-5 lesions by lesion size based on the original LI-RADS v2018 and modified LI-RADS

	Lesion size 10–19 mm (n = 65)										Lesion size ≥20 mm (n = 185)									
	Sensitivity (%)	Specificity (%)	Accuracy (%)	FNR (%)	FPR (%)	PPV (%)	NPV (%)	Sensitivity (%)	Specificity (%)	Accuracy (%)	FNR (%)	FPR (%)	PPV (%)	NPV (%)						
LI-RADS v2018	64.1 (25/39)	96.15 (25/26)	76.92 (50/65)	36 (14/39)	3.85 (1/26)	96.15 (25/26)	64.10 (25/39)	81.53 (128/157)	96.43 (27/28)	83.78 (155/185)	18.47 (29/157)	3.57 (1/28)	99.22 (128/129)	48.21 (27/56)						
LI-RADS-m1	79.49 (31/39)	96.15 (25/26)	86.15 (56/65)	20.51 (8/39)	3.85 (1/26)	96.88 (31/32)	75.76 (25/33)	83.44 (131/157)	96.43 (27/28)	85.41 (158/185)	16.56 (26/157)	3.57 (1/28)	99.24 (131/132)	50.94 (27/53)						
LI-RADS-m2	79.49 (31/39)	96.15 (25/26)	86.15 (56/65)	20.51 (8/39)	3.85 (1/26)	96.88 (31/32)	75.76 (25/33)	83.44 (131/157)	96.43 (27/28)	85.41 (158/185)	16.56 (26/157)	3.57 (1/28)	99.24 (131/132)	50.94 (27/53)						
<i>p</i> *	0.031	1.000						0.25	1.000											

**p* values, LI-RADS-m1 and LI-RADS-m2 compared with LI-RADS v2018 using McNemar’s test

Numbers in parentheses were used to calculate percentages

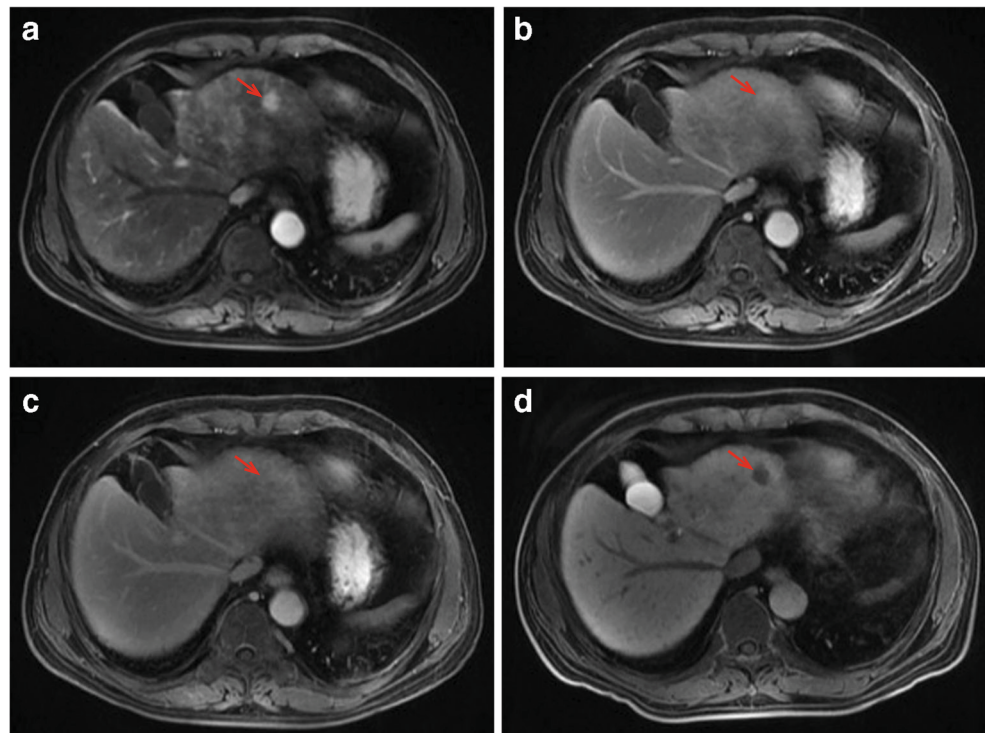
HCC, hepatocellular carcinoma; LI-RADS, Liver Imaging Reporting and Data System; LI-RADS-m1, modified LI-RADS by adding HBP hypointensity as a major feature; LI-RADS-m2, modified LI-RADS by replacing enhancing capsule with HBP hypointensity as the major feature; FNR, false-negative rate; FPR, false-positive rate; PPV, positive predictive value; NPV, negative predictive value

pseudocapsule due to contrast agent retention in the peritumoral hepatic sinusoids [33, 35]. This is important in that capsules are not always present or visible [21, 36]. Although capsule presence has been reported as a characteristic finding of HCC with a specificity of up to 96%, it usually coincides with the already typical dynamic radiological hallmarks (arterial enhancement followed by washout) [20, 21, 34]. This may limit its role in increasing diagnostic sensitivity. In addition, even for experienced experts in liver MRI diagnosis, the interobserver agreement regarding the enhancing capsule appearance is frequently moderate or low [7, 23, 24]. This may be a more serious problem than its diagnostic performance. In this study, interobserver agreement for the detection of enhancing capsule was moderate. Therefore, if enhancing capsule is used for diagnosis, the incremental diagnostic performance of this feature for LI-RADS categorization is limited.

Our subgroup analysis revealed a higher proportion of smaller (10–19 mm) lesions correctly classified as LR-5 with the addition of hypointensity in the HBP than larger (≥ 20 mm) lesions. One possible reason for this difference in our study may be the higher proportion of hypointense lesions in the HBP (36/36, 100%) than lesions with enhancing capsule (15/36, 42%) in smaller (10–19 mm) HCCs. In contrast, these features occurred with similar frequency (78% vs. 94%) in nodules that were 20 mm or larger. Furthermore, in this study, most lesions 20 mm or larger in size with an enhancing capsule already presented contrast washout (116/126, 92%). Regardless of the enhancing capsule, such lesions with non-rim APHE were already categorized as LR-5 according to the LI-RADS v2018 lexicon. This may explain the different diagnostic sensitivity for HCCs between 10–19 mm and ≥ 20 mm in size in our study. These results imply that this additional imaging sequence may be especially beneficial for the early detection of HCC in high-risk patients. In addition, lesion hypointensity in the HBP might be particularly advantageous for the characterization of small lesions in which an enhancing capsule is not visible.

Our study has some limitations. First, it was a retrospective, single-center study rather than a large-scale, prospective, multicenter study. A larger prospective multicenter study is warranted to verify our results. Second, we did not obtain histopathological confirmation for all benign nodules detected in our study. However, we employed strict criteria for the diagnosis of benign lesions, including follow-up imaging for at least 24 months. Third, the number of non-HCC lesions included in the study was relatively low. This reflects the fact that the patient population studied were those at increased risk for HCC; most nodules detected in patients at risk for HCC are, in fact, HCC. Further work in a more diverse lesion population with a larger number of non-HCC lesions is warranted to validate our findings. In this regard, it should also be noted that most patients in our population had chronic hepatitis B as the underlying clinical risk factor for HCC. This is

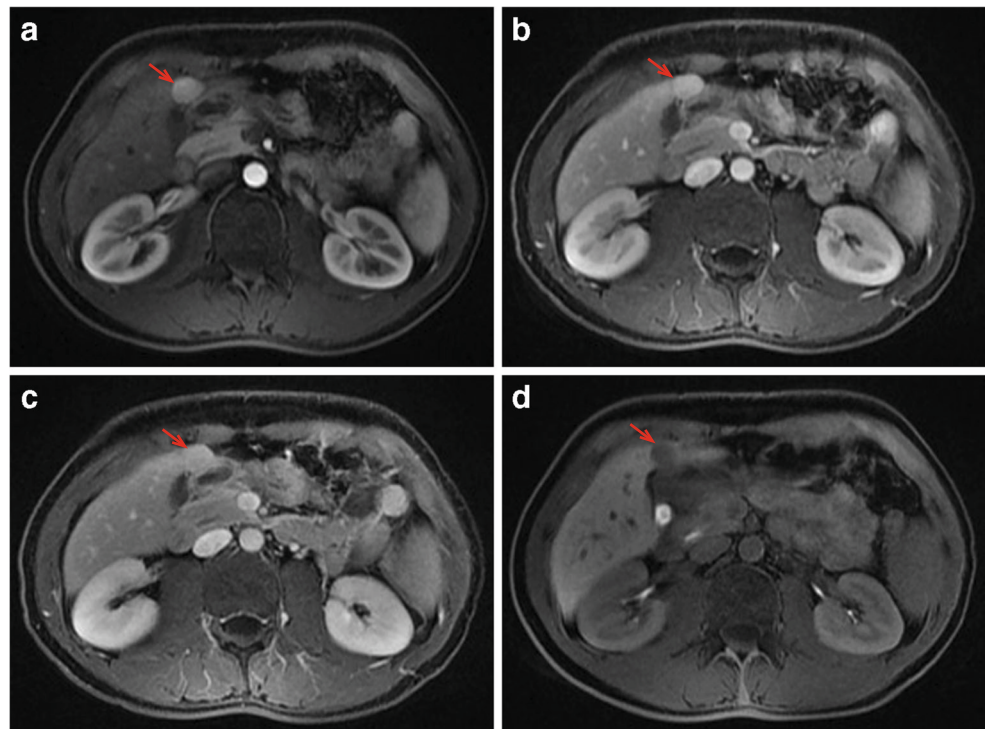
Fig. 2 A 62-year-old man with hepatitis B virus infection and surgically confirmed hepatocellular carcinoma in segment II (arrow in **a–d**). Gadobenate dimeglumine-enhanced MRI revealed a 16-mm lesion with hyperenhancement in the arterial phase (**a**), without washout and enhancing capsule in the portal-venous phase (**b**) and delayed phase (**c**). The lesion was hypointense in the hepatobiliary phase (HBP) (**d**). The lesion was classified as LR-3 based on LI-RADS v2018 criteria. However, when using HBP hypointensity to replace enhancing capsule as a major feature (LI-RADS-m2), the lesion was classified as LR-5



more representative of an East Asian population than a Western population. Therefore, further work is also needed to confirm our findings in patients with other forms of chronic liver disease, particularly cirrhosis. Finally, recent studies suggest that spectral detector CT-derived virtual monoenergetic

images may improve the washout assessment of hyperenhanced liver lesions in the arterial phase [37, 38]. Therefore, further work should also focus on the comparison of MRI and spectral detector CT for non-invasive detection and diagnosis of liver lesions in patients at high risk of HCC.

Fig. 3 A 36-year-old man with hepatitis B virus infection and surgically confirmed hepatocellular carcinoma in segment IV (arrow in **a–d**). Gadobenate dimeglumine-enhanced MRI revealed an 18-mm lesion with hyperenhancement in the arterial phase (**a**), without obvious washout and enhancing capsule in the portal-venous phase (**b**) and delayed phase (**c**). The lesion was hypointense in the hepatobiliary phase (HBP) (**d**). The lesion was classified as LR-3 based on LI-RADS v2018 criteria. However, when using HBP hypointensity to replace enhancing capsule as a major feature (LI-RADS-m2), the lesion was classified as LR-5



In conclusion, lesion hypointensity in the HBP increases the sensitivity for the diagnosis of LR-5 lesions based on LI-RADS v2018 criteria and can substitute for enhancing capsule as an additional major feature without decreasing specificity. Whereas HBP images are not always required for the characterization of HCC and non-HCC lesions [27], the availability of this additional imaging sequence on gadobenate-enhanced MRI can be considered a benefit for at-risk patients suspected of harboring HCC.

Supplementary Information The online version contains supplementary material available at <https://doi.org/10.1007/s00330-021-07807-y>.

Funding The authors state that this study has received funding from the National Natural Science Foundation of China grant 91959118 (JW), Science and Technology Program of Guangzhou, China grant 201704020016 (JW), SKY Radiology Department International Medical Research Foundation of China Z-2014-07-1912-15 (JW), and Clinical Research Foundation of the 3rd Affiliated Hospital of Sun Yat-sen University YHJH201901 (JW).

Compliance with ethical standards

Guarantor The scientific guarantor of this publication is Jin Wang.

Conflict of interest The authors of this manuscript declare no relationships with any companies whose products or services may be related to the subject matter of the article.

Statistics and biometry No complex statistical methods were necessary for this paper.

Informed consent Written informed consent was waived by the Institutional Review Board.

Ethical approval Institutional Review Board approval was obtained.

Methodology

- Retrospective
- Diagnostic or prognostic study
- Performed at one institution

References

- Marrero JA, Kulik LM, Sirlin CB et al (2018) Diagnosis, staging, and management of hepatocellular carcinoma: 2018 practice guidance by the American Association for the Study of Liver Diseases. *Hepatology* 68:723–750
- Heimbach JK, Kulik LM, Finn RS et al (2018) AASLD guidelines for the treatment of hepatocellular carcinoma. *Hepatology* 67:358–380
- European Association for the Study of the Liver (2018) EASL clinical practice guidelines: management of hepatocellular carcinoma. *J Hepatol* 69:182–236
- Cabibbo G, Anea M, Attanasio M, Bruix J, Craxi A, Cammà C (2010) A meta-analysis of survival rates of untreated patients in randomized clinical trials of hepatocellular carcinoma. *Hepatology* 51:1274–1283
- American College of Radiology (2018) Liver Imaging Reporting and Data System version 2018. Available via <http://www.acr.org/Quality-Safety/Resources/LIRADS>. Accessed 1 Jan 2020
- Alenazi AO, Elsayes KM, Marks RM et al (2020) Clinicians and surgeon survey regarding current and future versions of CT/MRI LI-RADS. *Abdom Radiol (NY)* 45:2603–2611
- Chernyak V, Fowler KJ, Kamaya A et al (2018) Liver Imaging Reporting and Data System (LI-RADS) Version 2018: imaging of hepatocellular carcinoma in at-risk patients. *Radiology* 289:816–830
- Cerny M, Chernyak V, Olivieri D et al (2018) LI-RADS Version 2018 Ancillary Features at MRI. *Radiographics* 38:1973–2001
- Bolondi L, Gaiani S, Celli N et al (2005) Characterization of small nodules in cirrhosis by assessment of vascularity: the problem of hypovascular hepatocellular carcinoma. *Hepatology* 42:27–34
- Forner A, Vilana R, Ayuso C et al (2008) Diagnosis of hepatic nodules 20 mm or smaller in cirrhosis: prospective validation of the noninvasive diagnostic criteria for hepatocellular carcinoma. *Hepatology* 47:97–104
- Renzulli M, Biselli M, Brocchi S et al (2018) New hallmark of hepatocellular carcinoma, early hepatocellular carcinoma and high-grade dysplastic nodules on Gd-EOB-DTPA MRI in patients with cirrhosis: a new diagnostic algorithm. *Gut* 67:1674–1682
- Sano K, Ichikawa T, Motosugi U et al (2011) Imaging study of early hepatocellular carcinoma: usefulness of gadoxetic acid-enhanced MR imaging. *Radiology* 261:834–844
- De Gaetano AM, Catalano M, Pompili M et al (2019) Critical analysis of major and ancillary features of LI-RADS v2018 in the differentiation of small (≤ 2 cm) hepatocellular carcinoma from dysplastic nodules with gadobenate dimeglumine-enhanced magnetic resonance imaging. *Eur Rev Med Pharmacol Sci* 23:7786–7801
- Song JS, Choi EJ, Hwang SB, Hwang HP, Choi H (2019) LI-RADS v2014 categorization of hepatocellular carcinoma: Intraindividual comparison between gadopentetate dimeglumine-enhanced MRI and gadoxetic acid-enhanced MRI. *Eur Radiol* 29:401–410
- Lee YJ, Lee JM, Lee JS et al (2015) Hepatocellular carcinoma: diagnostic performance of multidetector CT and MR imaging—a systematic review and meta-analysis. *Radiology* 275:97–109
- Cortis K, Liotta R, Miraglia R, Caruso S, Tuzzolino F, Luca A (2016) Incorporating the hepatobiliary phase of gadobenate dimeglumine-enhanced MRI in the diagnosis of hepatocellular carcinoma: increasing the sensitivity without compromising specificity. *Acta Radiol* 57:923–931
- Joo I, Lee JM, Lee DH, Jeon JH, Han JK (2019) Retrospective validation of a new diagnostic criterion for hepatocellular carcinoma on gadoxetic acid-enhanced MRI: can hypointensity on the hepatobiliary phase be used as an alternative to washout with the aid of ancillary features? *Eur Radiol* 29:1724–1732
- Joo I, Lee JM, Lee DH, Jeon JH, Han JK, Choi BI (2015) Noninvasive diagnosis of hepatocellular carcinoma on gadoxetic acid-enhanced MRI: can hypointensity on the hepatobiliary phase be used as an alternative to washout? *Eur Radiol* 25:2859–2868
- Kim DH, Choi SH, Kim SY, Kim M-J, Lee SS, Byun JH (2019) Gadoxetic acid-enhanced MRI of hepatocellular carcinoma: value of washout in transitional and hepatobiliary phases. *Radiology* 291:651–657
- Fowler KJ, Sirlin CB (2019) Is it time to expand the definition of washout appearance in LI-RADS? *Radiology* 291:658–659
- Rimola J, Forner A, Tremosini S et al (2012) Non-invasive diagnosis of hepatocellular carcinoma ≤ 2 cm in cirrhosis. Diagnostic accuracy assessing fat, capsule and signal intensity at dynamic MRI. *J Hepatol* 56:1317–1323
- Chung JW, Yu J-S, Choi JM, Cho E-S, Kim JH, Chung J-J (2020) Subtraction images from portal venous phase gadoxetic acid-

- enhanced MRI for observing washout and enhancing capsule features in LI-RADS Version 2018. *AJR Am J Roentgenol* 214:72–80
23. Ehman EC, Behr SC, Umetsu SE et al (2016) Rate of observation and inter-observer agreement for LI-RADS major features at CT and MRI in 184 pathology proven hepatocellular carcinomas. *Abdom Radiol (NY)* 41:963–969
 24. Sofue K, Sirlin CB, Allen BC, Nelson RC, Berg CL, Bashir MR (2016) How reader perception of capsule affects interpretation of washout in hypervascular liver nodules in patients at risk for hepatocellular carcinoma. *J Magn Reson Imaging* 43:1337–1345
 25. Spinazzi A, Lorusso V, Pirovano G, Kirchin M (1999) Safety, tolerance, biodistribution, and MR imaging enhancement of the liver with gadobenate dimeglumine: results of clinical pharmacologic and pilot imaging studies in nonpatient and patient volunteers. *Acad Radiol* 6:282–291
 26. Morana G, Grazioli L, Kirchin MA et al (2011) Solid hypervascular liver lesions: accurate identification of true benign lesions on enhanced dynamic and hepatobiliary phase magnetic resonance imaging after gadobenate dimeglumine administration. *Invest Radiol* 46:225–239
 27. Grazioli L, Morana G, Kirchin MA, Schneider G (2005) Accurate differentiation of focal nodular hyperplasia from hepatic adenoma at gadobenate dimeglumine-enhanced MR imaging: prospective study. *Radiology* 236:166–177
 28. Zhang L, Yu X, Huo L et al (2019) Detection of liver metastases on gadobenate dimeglumine-enhanced MRI: systematic review, meta-analysis, and similarities with gadoxetate-enhanced MRI. *Eur Radiol* 29:5205–5216
 29. Duncan JK, Ma N, Vreugdenburg TD, Cameron AL, Maddern G (2017) Gadoxetic acid-enhanced MRI for the characterization of hepatocellular carcinoma: a systematic review and meta-analysis. *J Magn Reson Imaging* 45:281–290
 30. Allen BC, Ho LM, Jaffe TA, Miller CM, Mazurowski MA, Bashir MR (2018) Comparison of visualization rates of LI-RADS version 2014 major features with IV gadobenate dimeglumine or gadoxetate disodium in patients at risk for hepatocellular carcinoma. *AJR Am J Roentgenol* 210:1266–1272
 31. Frydrychowicz A, Nagle SK, D'Souza SL, Vigen KK, Reeder SB (2011) Optimized high-resolution contrast-enhanced hepatobiliary imaging at 3 tesla: a cross-over comparison of gadobenate dimeglumine and gadoxetic acid. *J Magn Reson Imaging* 34:585–594
 32. Burgio MD, Picone D, Cabibbo G, Midiri M, Lagalla R, Brancatelli G (2016) MR-imaging features of hepatocellular carcinoma capsule appearance in cirrhotic liver: comparison of gadoxetic acid and gadobenate dimeglumine. *Abdom Radiol (NY)* 41:1546–1554
 33. Ishigami K, Yoshimitsu K, Nishihara Y et al (2009) Hepatocellular carcinoma with a pseudocapsule on gadolinium-enhanced MR images: correlation with histopathologic findings. *Radiology* 250:435–443
 34. Kadoya M, Matsui O, Takashima T, Nonomura A (1992) Hepatocellular carcinoma: correlation of MR imaging and histopathologic findings. *Radiology* 183:819–825
 35. Lee SE, An C, Hwang SH, Choi J-Y, Han K, Kim M-J (2018) Extracellular contrast agent-enhanced MRI: 15-min delayed phase may improve the diagnostic performance for hepatocellular carcinoma in patients with chronic liver disease. *Eur Radiol* 28:1551–1559
 36. Khan AS, Hussain HK, Johnson TD, Weadock WJ, Pelletier SJ, Marrero JA (2010) Value of delayed hypointensity and delayed enhancing rim in magnetic resonance imaging diagnosis of small hepatocellular carcinoma in the cirrhotic liver. *J Magn Reson Imaging* 32:360–366
 37. Reimer RP, Hokamp NG, Efferoth AF et al (2020) Virtual monoenergetic images from spectral detector computed tomography facilitate washout assessment in arterially hyperenhancing liver lesions. *Eur Radiol*. <https://doi.org/10.1007/s00330-020-07379-3>
 38. Hokamp NG, Höink AJ, Doerner J et al (2018) Assessment of arterially hyper-enhancing liver lesions using virtual monoenergetic images from spectral detector CT: phantom and patient experience. *Abdom Radiol (NY)* 43:2066–2074

Publisher's note Springer Nature remains neutral with regard to jurisdictional claims in published maps and institutional affiliations.